Journal of Medicinal Chemistry

ARTICLE

pubs.acs.org/jmc

Imidazolopiperazines: Hit to Lead Optimization of New Antimalarial Agents

Tao Wu,[†,#] Advait Nagle,[†,#] Kelli Kuhen,[†] Kerstin Gagaring,[†] Rachel Borboa,[†] Caroline Francek,[†] Zhong Chen,[†] David Plouffe,[†] Anne Goh,[§] Suresh B. Lakshminarayana,[§] Jeanette Wu,[§] Hui Qing Ang,[§] Peiting Zeng,[§] Min Low Kang,[§] William Tan,[§] Maria Tan,[§] Nicole Ye,[§] Xuena Lin,[⊥] Christopher Caldwell,[⊥] Jared Ek,[†] Suzanne Skolnik,[⊥] Fenghua Liu,[⊥] Jianling Wang,[⊥] Jonathan Chang,[†] Chun Li,[†] Thomas Hollenbeck,[†] Tove Tuntland,[†] John Isbell,[†] Christoph Fischli,[‡,∥] Reto Brun,[‡,∥] Matthias Rottmann,[‡,∥] Veronique Dartois,[§] Thomas Keller,[§] Thierry Diagana,[§] Elizabeth Winzeler,[†] Richard Glynne,[†] David C. Tully,[†] and Arnab K. Chatterjee*[,†]

[†]Genomics Institute of the Novartis Research Foundation, 10675 John Jay Hopkins Drive, San Diego, California 92121, United States

[‡]Swiss Tropical and Public Health Institute, Parasite Chemotherapy, Socinstrasse 57, Basel, Switzerland CH-4002

[§]Novartis Institute for Tropical Diseases, 10 Biopolis Road, no. 05-01 Chromos, Singapore 138670

[∥]University of Basel, Petersplatz 1, Basel, Switzerland CH-4003

[⊥]Novartis Institute for Biomedical Research, Preclinical Profiling Group, Cambridge, Massachusetts, United States

ABSTRACT: Starting from a hit series from a GNF compound library collection and based on a cell-based proliferation assay of *Plasmodium falciparum*, a novel imidazolopiperazine scaffold was optimized. SAR for this series of compounds is discussed, focusing on optimization of cellular potency against wild-type and drug resistant parasites and improvement of physiochemical and pharmacokinetic properties. The lead compounds in this series showed good potencies in vitro and decent oral exposure levels in vivo. In a *Plasmodium berghei* mouse infection model, one lead compound lowered the parasitemia level by 99.4% after administration of 100 mg/kg single oral dose and prolonged mice survival by an average of 17.0 days. The lead compounds were also well-tolerated in the preliminary *in vitro* toxicity studies and represents an interesting lead for drug development.

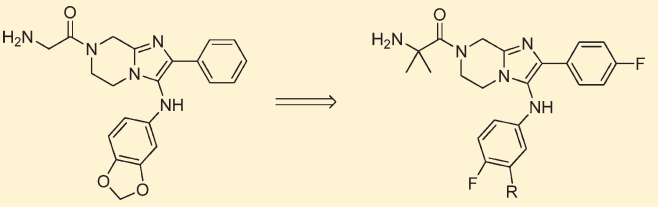

INTRODUCTION

After thousands of years, malaria is still one of the major infectious diseases that affect millions of people, especially those in underdeveloped countries.[1] In the absence of effective antimalarial vaccines, low molecular weight antimalarial drugs are important weapons against the disease.[2] Quinine, chloroquine, mefloquine, and artemisinin derivatives have played an important role in fighting against malaria. However, widespread drug resistance has made them less effective with artemisinin derivatives as the only exception. Artemisinin based combination therapies (ACT) recommended by WHO will help to delay the emergence of clinical resistance against artemisinins, but reports of increased parasite clearance times have emerged recently.[3] Therefore, it is important to discover antimalarials with novel chemical entities that are effective against the multidrug resistant parasite strains. Here we report our continued effort to develop novel antimalarials from a cell-based screening strategy.[4]

In our quest to discover novel chemotypes that inhibit *Plasmodium falciparum*, we previously disclosed a more extensive screening campaign on a library of about 2 million compounds using a cell-based proliferation assay of *Plasmodium falciparum* (strain 3D7).[5] Five-thousand of the reconfirmed hits have been subsequently disclosed in a public malaria database (see https://www.ebi.ac.uk/chembldb/index.php), and we analyzed the hit list with the following criteria: (1) good potency, where IC_{50} values were less than 1 μM against wild type as well as drug resistant strain; (2) good safety index, greater than 20-fold in a six-cell line toxicity panel; (3) easy synthesis and preferably with multiple active hits within the scaffold.

Compounds **1a**−**c** consisting of imidazolopiperazine moiety presented themselves as an attractive hit series based on these criteria (Table 1). Their structures were distinct from the current known antimalarials such as aminoquinolines and endo-peroxides. Compounds **1a**−**c** represented decent starting points in terms of potency in both wild type and drug resistant strain, and the scaffold exhibited a high selectivity index (>20-fold) against Huh7 cell line. Moreover, one of the representative compound,

Received: March 22, 2011
Published: June 06, 2011

   dx.doi.org/10.1021/jm2003359 | *J. Med. Chem.* 2011, 54, 5116–5130

Table 1. Structures of Hits from the HTS Screen

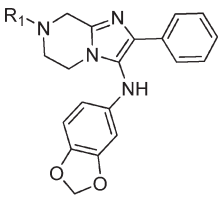

1(a-c)

			P. falciparum strain IC_{50} [a] (nM)		
					cytotoxicity (μM)
compd	EBI code	R_1	3D7	W2	Huh7
1a	GNF-Pf-5069	Gly	63 [460]	97 [473]	>10 [>100]
1b	GNF-Pf-5179	(DL)-Phe	235 [119]	271 [122]	>10 [>79]
1c	GNF-Pf-5466	(DL)-Leu	116 [30]	119 [29]	>10 [42]

[a] Values are the mean of at least two experiments. Data in brackets are for resynthesized powders; otherwise data are from HTS DMSO stock solutions.

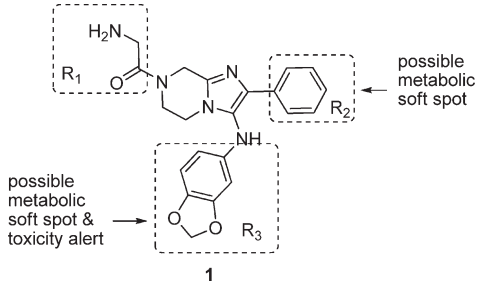

Figure 1. Initial hit of imidazolopiperazine series and plans to optimize the three peripheral parts.

1a, was highly soluble (>175 μM at pH 6.8) and clean on most commonly drug affected cytochrome P450 isoforms (IC_{50} values were greater than 10 μM for CYP1A2, CYP2C19, CYP2C9, CYP2D6, and CYP3A4). Despite the basic amine functionality on R_1, compound **1a** was a moderate hERG substrate as determined by binding assay (IC_{50} = 19 μM, 57% inhibition at 10 μM). However, compound **1a** exhibited poor plasma oral exposure with C_{max} = 320 nM and $AUC_{(0-5h)}$ = 972 (h·nM) in an oral mouse snapshot PK study, indicating the presence of metabolic soft spots within the molecule or overall poor permeability properties.[6]

The major goal of optimization was to improve potency and remove metabolically vulnerable functionality of the compounds. Figure 1 shows our initial objectives. In line with the three possible metabolic soft spots of compound **1a**, we decided to study the three peripheral sections: the amino acid moiety R_1, the phenyl moiety R_2, and the aniline moiety R_3. We hoped changes in these parts would help us deliver a candidate with enhanced potency as well as improved oral exposure.

CHEMISTRY

The synthesis of imidazolopiperazine compounds such as **5** is outlined in Scheme 1. A Groebke–Blackburn three-component reaction of 2-aminopyrazine with 4-fluorophenyl isocyanide and 4-fluorobenzaldehyde efficiently furnished the skeleton.[7] A PtO_2 mediated reduction of the pyrazine ring then afforded desired core structure.[8] Compound **5** was obtained by a HATU mediated amidation reaction with *N*-Boc-glycine followed by a TFA mediated deprotection of the amino group. When not commercially available, isocyanides were prepared in a formylation–dehydration sequence from the corresponding anilines.[8]

To efficiently evaluate the R_3 section and avoid repeated preparation and usage of notoriously noxious isocyanides, compound **6** was prepared from the same Groebke–Blackburn three-component reaction of 2-aminopyrazine with *tert*-butyl isocyanide and 4-fluorobenzaldehyde. After removal of the *tert*-butyl group, the obtained compound **7** was then used as a common intermediate. A palladium mediated amination with different aryl bromides provided various analogues of compound **7**.[9]

RESULTS AND DISCUSSION

Structure–Activity Relationship. The potency of the compounds was determined against the 3D7 and W2 multidrug resistant strains using Sybergreen assay previously described in our HTS disclosure (Table 2).[5] Each assay plate had mefloquine and artemisinin as standards to ensure the reliability of the assay. We decided to (1) test various natural and unnatural amino acids on R_1, (2) add substituents to the right side phenyl ring, and (3) replace the methylenedioxyl moiety with substituted phenyl rings, heterocycles, and aliphatic rings. We began exploring the SAR studies on the initial hit compounds **1a–c** by determining the minimal pharmacophore needed for the antiplasmodial activity. On the basis of the preliminary results, it was clear that dearomatized compound **3** provided us with a decent starting point for further SAR exploration on all the three parts of the molecule. Installation of a glycine group gave us compound **5**, which was 4-fold more potent than the original hit compound **1a**. On the basis of this result, we focused our efforts on evaluating various amino acids. Increasing the chain length of the amino acid moiety led to **8**, which had inferior activity. Various monosubstitution on the α position provided potent compounds (compounds **9**, **10**, **12**, and **13**) which were less than 100 nM in potency range. The testing of both of the enantiomers of phenylalanine derivatives indicated that the stereochemistry of the amino acid moiety was not important. Removal of chiral center from compound **9** led us to α-methylalanine derivative **11**.

dx.doi.org/10.1021/jm2003359 |*J. Med. Chem.* 2011, 54, 5116–5130

Scheme 1. Representative Synthetic Route of Imidazolopiperazines[a]

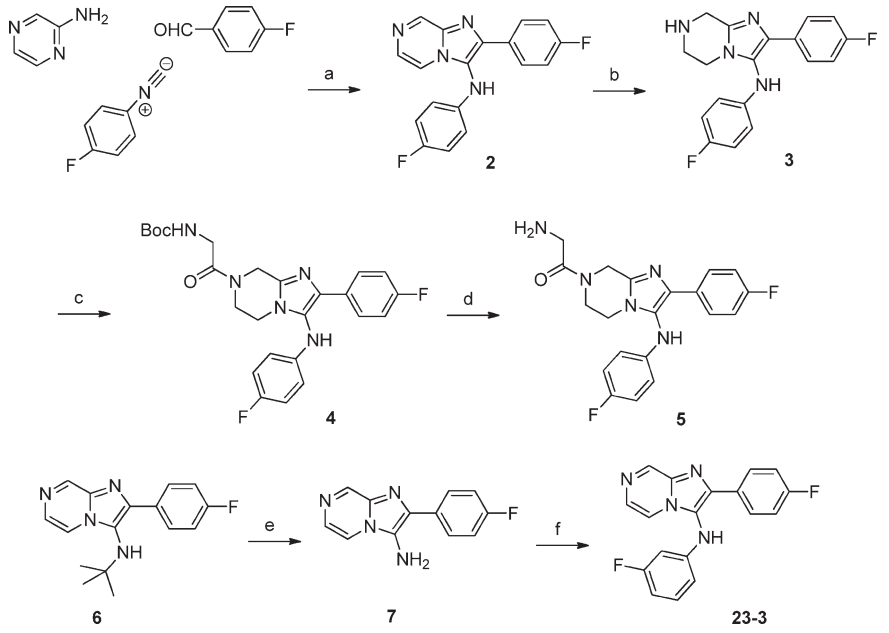

[a] Reagents and conditions: (a) $HClO_4$, MeOH, room temp, 48%; (b) PtO_2, H_2 (balloon), MeOH, room temp, quantitative; (c) *N*-Boc-glycine, HATU, DIEA, DMF, room temp, 72%; (d) TFA, DCM, room temp, quantitative; (e) TFA, DCM, room temp, quantitative; (f) 1-bromo-3-fluorobenzene, $Pd_2(dba)_3$, Xantphos, Cs_2CO_3, dioxane, 150 °C, 66%.

This compound had a decent activity of 20 nM against the parasites but offered an enormous advantage of blocking a potential metabolic soft spot and removing chirality in the molecule. A number of second and tertiary amines on the amino acid side chain had deleterious effects on the potency (compounds not shown). The future analogues were optimized using glycine or α-methylalanine as the side chain.

The study of the R_2 group revealed that this portion of the molecule was not amenable to broad changes (Table 3). Compounds **5**, **14**, and **15** indicated that only small size substituents such as fluorine or hydrogen were tolerated. A comparison of compounds **5**, **18**, and **19** indicated that para and meta substitutions were tolerated but not ortho substitution. 3,4-Difluoro substitution (compound **20**) did not provide additional boost in potency, and hence, it was inferred that 4-fluoro substitution provided the best atom economy for further SAR optimization. Attempts to replace the phenyl ring with a cyclohexyl group led to total loss in potency (compound not shown).

After optimizing the R_1 and R_2 groups, we focused our attention on the aniline portion of the molecule (Table 4). One general trend was that compounds with glycine as R_1 were usually more potent than their counterparts with dimethylglycine as R_1. The potencies for compounds **21** and **22** indicated that aliphatic rings and heterocyclic rings were not tolerated. A number of different substituents (compounds **23**−**28**) at either meta or para position gave active compounds. With the same substituents, 3,4-disubstitution was preferred over 2,4-disubsitution and 3,5-disubstitution patterns (compounds **33** and **34**). The most potent compound was **31**, which exhibited an EC_{50} of 3 nM on 3D7 and of 4 nM on W2.

ADMET and Pharmacokinetic Properties. Along with the extensive SAR study to optimize the potency of this series, some of the more potent analogues in different categories were evaluated for their in vitro ADME and in vivo pharmacokinetic properties. In general, this series of compounds had very good

Table 2. SAR Study of R_1 Moiety

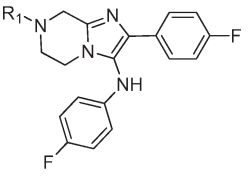

		P. falciparum strain IC_{50}[a] (nM)	
compd	R_1	3D7	W2
2		>10	5520
3	H	200	175
5	Gly	20	23
8	*β*-Ala	70	75
9	(L)-Ala	90	64
10	(L)-Val	30	24
11	α-Me-Ala	20	25
12	(L)-Phe	110	121
13	(D)-Phe	70	59
	mefloquine	12	8
	pyrimethamine	29	>10000
	artemisnin	12	14

[a] Values are the mean of at least two experiments.

Lipinski's rule-of-five compliance and most of the analogues were highly soluble (>175 μM at pH 6.8).

Table 5 summarizes the in vitro ADMET profiles of compounds with good in vitro potency. In general, metabolic stability of the compounds was good to moderate across three species, with rat being the most sensitive species and thus exhibiting the highest hepatic extraction ratio (ER). One interesting finding was

dx.doi.org/10.1021/jm2003359 |*J. Med. Chem.* 2011, 54, 5116–5130

Table 3. SAR Study of R_2 Moiety

compd	R_1	R_2	*P. falciparum* strain IC_{50}[a] (nM) 3D7	W2
14	α-Me-Ala	Ph	200	168
15	Gly	4Cl-Ph	660	437
16	Gly	4OMe-Ph	2270	1702
17	Gly	4Me-Ph	3140	3360
18	Gly	3F-Ph	10	30
19	α-Me-Ala	2F-Ph	1390	1284
20[b]	α-Me-Ala	3F,4F-Ph	60	50

[a] Values are the mean of at least two experiments. [b] Compound with 4-methylphenyl as R_3.

Table 4. SAR Study of R_3 Moiety

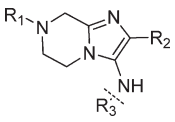

compd	R_1	R_2	R_3	IC_{50}[a] (nM) 3D7	W2
21	α-Me-Ala	4F-Ph	cyclohex-	9610	5980
22	α-Me-Ala	4F-Ph	3-pyridine	1413	3320
23	Gly	4F-Ph	3F-Ph	50	34
24	α-Me-Ala	3F-Ph	4F-Ph	50	71
25	Gly	4F-Ph	4Me-Ph	10	13
26	α-Me-Ala	4F-Ph	4Me-Ph	20	24
27	Gly	4F-Ph	4Cl-Ph	10	9
28	α-Me-Ala	4F-Ph	4Cl-Ph	30	24
29	Gly	4F-Ph	3F,4F-Ph	30	23
30	α-Me-Ala	4F-Ph	3F,4F-Ph	44	36
31	Gly	4F-Ph	3F,4Cl-Ph	3	4
32	α-Me-Ala	4F-Ph	3F,4Cl-Ph	40	52
33	α-Me-Ala	4F-Ph	2F,4F-Ph	110	90
34	α-Me-Ala	4F-Ph	3F,5F-Ph	220	244

[a] Values are the mean of at least two experiments.

that analogues with glycine as R_1 and analogues with dimethylglycine as R_1 behaved quite differently in terms of hERG activity. Although the glycine analogues offered a safety advantage in terms of low affinity to hERG channel, it was negated by low permeability, as indicated by PAMPA and Caco-2 assays. In general, this also led to lower bioavailability as discussed below. While the dimethylglycines indicated some efflux due to high B—A values, this generally did not lead to lower bioavailability, potentially indicating a saturation of efflux mechanism (such as p-glycoproteins) at the doses used in the oral PK studies.

The in vivo pharmacokinetic properties were studied in non-infected male balb/C or female CD-1 mice. The overall trend for the oral exposure was in line with the predictions from the permeability assays. Four pairs of head to head comparison (entry **11**/**5**, entry **18**/**24**, entry **25**/**26**, and entry **31**/**32**) of the oral arm C_{max}, AUC, and bioavailability revealed that dimethylglycine analogues generally had low hepatic in vivo clearance which resulted in higher AUCs as well as making the compounds more orally available (Table 6). Upon comparison of the pharmacokinetic profiles (Figure 2) for both compounds, it was observed that compound **32** has much higher exposure in the oral arm whereas the intravenous kinetics were comparable for both molecules (graph for compound **31** not shown for clarity). Some of the tested compounds exhibited high volume of distribution (>10 L/kg) and high plasma clearance (>90 (mL/min)/kg) in mice. On the basis of data from in vitro mouse blood to plasma partitioning of structural analogues with blood to plasma ratio of >1, these compounds might be partitioned into red blood cells leading to overestimation of blood clearance and extent of tissue distribution.

In Vivo Efficacy. The in vivo antimalarial activities of the optimized compounds were evaluated using a *Plasmodium berghei* mouse model.[10] In this test, groups of three *P. berghei* infected mice were treated orally with compound starting 1 day after infection. The key readouts were the percentage of parasitemia reduction on day 3 postinfection (day 4 postinfection in the case of a 3-day treatment schedule) compared to the untreated mice and the prolongation of survival of the infected mice.

Table 7 summarized the in vivo efficacy test results of selected compounds compared with the standard antimalarials chloroquine (CQ) and artesunate (AS). At 1 × 100 mg/kg dose level, most of the compounds could reduce the parasitemia for more than 99% and prolong mice survival for more than 10 days. Interestingly, for the three head-to-head comparison pairs (entry **25**/**26**, entry **31**/**32**, and entry **18**/**24**), the glycine analogues were less efficacious at 1 × 100 and 1 × 30 mg/kg dose levels despite their better potencies. It was likely that the better oral exposure of the dimethylglycine analogues is responsible for this outcome. Among all the tested compounds, compounds **11** and **30** stood out as the most efficacious compounds at 1 × 100 and 1 × 30 mg/kg dose levels. They both showed parasitemia reduction activities and survival prolongation comparable those of CQ and AS. When the 1 × 30 mg/kg and 3 × 30 mg/kg dose levels are compared, both compounds **11** and **30** demonstrated improved efficacy.

In Vitro Toxicology. Because of their good in vitro potency and in vivo efficacy results, compounds **11** and **30** were evaluated for their toxicity profile. Both compounds did not inhibit cytochromes P450 isoforms (IC_{50} values were greater than 8.9 μM for CYP1A2, CYP2C19, CYP2C9, CYP2D6, and CYP3A4). The observed cytotoxicity TC_{50} values (293T, Ba/F3, CHO, HEp2, HeLa, Huh7) were all greater than 12 μM, which translates to a good selectivity index (SI > 100). Compound **11** was well tolerated in the maximum tolerable dose test in rats in vivo with no gross effects at doses up to 500 mg/kg. Compound **30** was negative in the mini-Ames and micronucleus tests. The only safety concern for these two lead compounds were their hERG liability. Although compounds **11** and **30** exhibited IC_{50} of 5.6 and 4.8 μM, respectively, there was a toxicity index of 100-fold when compared to the cellular potency against the parasites.

SUMMARY

A series of imidazolopiperazines was selected as one of the good hits from a high throughput screen of two million library compounds against a cell based parasite proliferation assay. After

dx.doi.org/10.1021/jm2003359 |J. Med. Chem. 2011, 54, 5116–5130

Table 5. In Vitro ADME of Selected Analogues[a]

compd	PAMPA (% absorbed)	Caco-2 A−B ($cm/s \times 10^6$)	Caco-2 B−A ($cm/s \times 10^6$)	hepatic microsome metabolic stability (extraction ratio)			hERG (Q-patch) IC_{50} (μM)
				mouse	rat	human	
5	52	0.70	2.55	0.47	nt	<0.21	nt
11	81	3.05	8.38	0.51	0.63	0.52	5.6
18	low	0.56	2.32	0.31	nt	nt	>30
24	92	1.07	2.6	0.46	nt	nt	5.7
25	52	1.63	3.58	0.17	nt	nt	11.1
26	96	0.96	1.66	0.19	0.87	0.54	1.5
27	52	0.44	1.25	0.17	0.63	0.55	nt
28	89	1.46	1.86	0.17	0.43	0.54	2.3
29	low	0.99	2.99	0.21	0.38	0.21	nt
30	86	0.14	1.03	0.17	0.12	0.39	4.8
31	low	0.75	0.96	0.57	0.6	0.37	21
32	94	0.84	0.87	0.76	0.67	0.48	5.6

[a] nt = not tested.

Table 6. In Vivo Pharmacokinetic Profile of Selected Analogues after Oral Dose at 30 mg/kg and iv Dose at 5 mg/kg in Mice[a]

compd	intravenous PK parameters				oral PK parameters				
	V_d (L/kg)	CL (mL/min/kg)	$T_{1/2}$ (h)	$AUC_{(inf)}$ (nM·h)	C_{max} (nM)	T_{max} (h)	$T_{1/2}$ (h)	$AUC_{(inf)}$ (nM·h)	F (%)
5	12.3	188.9	2.7	1072	234	2.0	4.2	965	15
11	23.7	60.0	6.2	3442	1803	1.67	9.0	17894	87
18	21.6	192.3	1.8	1232	417	2.0	1.0	1330	18
24	12.8	134.2	2.3	1319	778	0.50	2.3	3719	47
25	39.7	222.2	3.6	976	343	2.0	4.8	2343	40
26	41.1	42.0	13.7	5253	1007	2.0	15.5	17964	57
28	40.5	65.2	8.7	2985	749	1.00	37.6	28301	158
30	14.0	27.7	7.7	7003	1940	1.67	7.7	31758	76
31	1.5	10.3	3.8	20582	790	2.0	3.6	6175	5
32	1.7	5.8	7.8	25464	3319	2.0	9.1	36668	24

[a] Intravenous dosing was at 5 mg/kg. Compounds **11** and **30** were dosed at 20 mg/kg. PK values were normalized to 30 mg/kg for comparison. For compounds **11** and **30**: Species/strain, Balb/c mice. Formulation: 2.5 mg/mL in PEG300/D5W, 3:1, solution. All of the other compounds were dosed at 30 mg/kg po; strain, CD-1 female mice. Solution formulation with citrate buffer 50 mM (pH 4.5) for iv route and citrate buffer 100 mM (pH 3.5) for po route for compounds **5**, **18**, **24**, **25**, **26**, and **28**. Solution formulation for compounds **31** and **32**: Ethanol/PEG400/10% vitamin ETPGS (10:30:60) was used.

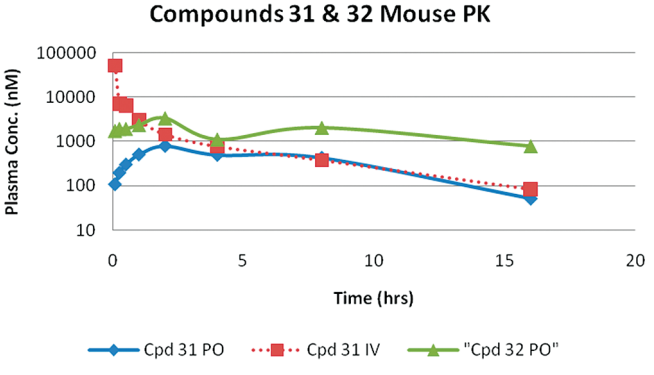

Figure 2. Graphical representation of po and iv kinetics for compounds **31** and **32**.

extensive optimization, the most potent compounds achieved single digit nanomolar range. The lead compounds showed good physicochemical and pharmacokinetic properties as well as safety profile. In the rodent *P. berghei* model, compounds **11** and **30** were as efficacious as the known antimalarials at 1 × 100 and 1 × 30 mg/kg dose levels.

The mechanism of actions for the imidazolopiperazine series is not clear. The tested compounds were active against 15 *Plasmodium falciparum* parasite strains with no potency shift, which proved their effectiveness against the existing multidrug resistant parasite stains. In a time when artemisinin based therapy is the last defense line for multidrug resistant malaria parasite strains, a novel effective chemical entity with distinct structure and mechanism of action will help to offer a new layer of protection. The continued optimization of this series will be reported in due course.

EXPERIMENTAL SECTION

Biology. Maintenance of *Plasmodium falciparum* Cultures. *Plasmodium falciparum* cultures are grown in O^+ RBCs using culturing medium: RPMI 1640 medium (no phenol red) with

dx.doi.org/10.1021/jm2003359 |J. Med. Chem. 2011, 54, 5116–5130

Table 7. In Vivo Efficacy of Selected Analogues on *P. berghei* Rodent Malaria Model after Different Dose Levels[a]

	1 × 30 mg/kg		1 × 100 mg/kg		3 × 30 mg/kg	
compd	parasitemia reduction (%)	survival (day)	parasitemia reduction (%)	survival (day)	parasitemia reduction (%)	survival (day)
11	99.3	7.7	99.6	13.3	99.9	14.0
18	86	6.0	99.7	10.0		
24	83	7.0	99.7	12.7		
25	83	6.3	99.6	10.3		
26	94	7.3	99.6	13		
28	98	6.0	99.5	13.0		
30[b]	99.4	7.7	99.4	17.0	99.8	17.7
31	77	6.7	99.6	9.0		
32	93	7.0	99.8	11.0		
CQ	99.7	8.7	>99.9	12	98.6	18.8
AS	89	7.2	97	6.7	98	7.2

[a] Activity = average parasitemia reduction. Survival = average lifespan after infection; 6−7 days for untreated mice; 7% Tween 80/3% ethanol formulation. [b] 75% PEG300/25%D5W formulation.

L-glutamine and containing 0.05 mg/mL gentamicin, 0.014 mg/mL hypoxanthine, 38.4 mM Hepes, 0.20% sodium bicarbonate, 0.20% glucose, 3.4 nM NaOH, 5% human serum, and 1.25% albumax. By use of traditional *P. falciparum* protocols published previously, 25 mL cultures are maintained in 75 cm^2 flasks (Fisher catalog no. 10-126-41) at 5% hematocrit and parasitemia ranging between 1% and 10%.[11] Once parasitemia reaches 8−10%, cultures are diluted to 1% or higher depending on needs. Maintenance requires daily medium changes and fresh blood every 2 weeks. Cultures are gassed for approximately 30 s to 1 min using a blood−gas mixture to maintain a gas composition of 96% nitrogen, 3% carbon dioxide, and 1% oxygen and incubated at 37 °C. On day 1 of the assay, percent parasitemia is determined by obtaining a 1 μL blood smear. The smear is fixed onto the slide by placing in methanol for 30 s and staining in 10% Geimsa stain, and the percent of parasitized erythrocytes vs uninfected erythrocytes is determined by microscopy with a light microscope.

Antimalarial Proliferation Inhibition Assay: 384-Well Plate Format. *P. falciparum* strains to be used for screening are prepared with screening medium (culturing medium without human serum but supplemented with 0.5% Albumax II) and fresh erythrocytes. An amount of 20 μL of screening medium is dispensed via the MicroFlo (BioTek) into 384-well, black clear-bottom assay plates (μClear GNF custom plates by Griener Bio-One). An amount of 50 nL of compounds is transferred using a PlateMate Plus (Matrix) or the GNF Systems PinTool into the assay plates containing screening medium to a final maximum concentration of 10 μM in a 12-point dose response (1/2 log serial dilution). On the basis of the measured parasitemia levels, each parasite strain is diluted to yield 0.5% parasitemia, and 50% hematocrit blood (uninfected erythrocytes) is added to a concentration of 4.17%. This diluted culture is used in dispensing the remaining 60% of the assay volume (30 μL) into the prewarmed assay plates via the MicroFlo liquid dispenser. The final parasitemia is 0.3% and the final hematocrit is 2.5% in a total volume of 50 μL. Assay plates are incubated at 37 °C for 72 h in a gas chamber filled with low oxygen blood gas. After the 72 h of incubation (equivalent to one to two cycles during the blood stage) a prepared mixture of the lysis buffer (5 mM EDTA, 1.6% Triton X-100, 20 mM Tris-HCl, 0.16% saponin) in water and SYBR Green detection (0.1%) reagent is dispensed at 10 μL per well using the MicroFlo. Cultures are incubated for an additional 24 h at 25 °C before measuring fluorescence intensity using the Envision plate reader (Perkin-Elmer) with a 505 dichroic mirror. Excitation and emission filters are 485 and 530 nm, respectively. Data are normalized based on maximum fluorescence signals for DMSO treated wells (no inhibition by compound) and the minimum fluorescence signals for wells containing the highest concentration of inhibitor control compounds, for pyrimethamine, at a final concentration of 10 μM. Data are analyzed on a plate-by-plate basis and compared to reference compounds that are always included on every plate, typically artemisinin, mefloquine, and pyrimethamine. EC_{50} values are obtained using a custom curve fitting model, and a standard logistic regression model is applied for curve fitting. The quality of the assay run is assessed by the performance of the reference compounds where the EC_{50} must be within 3-fold of the standard reference values for the assay plate to pass requisite data quality control needs. Additionally, all compounds are typically assayed at a minimum in duplicate (independent assay plates) and EC_{50} values ideally must not vary by more than 2-fold between plates.

Metabolic Stability. The metabolic stability of drug candidates is determined in human, mouse, and rat liver microsomes using the compound depletion approach, quantified by LC/MS/MS. The assay measures the rate and extent of metabolism of chemical compounds by measuring the disappearance of the parent compound. The assay determines the compound's in vitro half-life ($T_{1/2}$) and hepatic extraction ratios (ER) and predicts metabolic clearance in human, rat, and mouse species.[12]

Pampa Assay. Permeation experiments were carried out in 96-well microtiter filter plates. The compound concentration was determined by UV absorption measured with a SpectraMax190 microplate spectrophotometer (Molecular Devices Corporation, Sunnyvale, CA, U.S.) at absorption wavelengths between 260 and 290 nm.[13]

Caco-2 Assay. The Caco-2 assay was carried out in a 96-well format, and compound concentrations in each chamber are measured by LC/MS. The assay offers apparent permeability data of test compounds from the apical to the basolateral chambers [P_{app}(A−B)] and from the basolateral to the apical chambers [P_{app}(B−A)]. The results can be used to predict the in vivo oral absorption (using P_{app}(A−B)) and the transport mechanism of the test compounds across GI membrane (ratio P_{app}(B−A)/P_{app}(A−B) and log *P* lipophilicity data).[14]

hERG (Q-Patch) Assay. The assay utilizes electrophysiology measurements on the electric current passing through hERG channel that is heterologously expressed in a stable CHO cell line. Channels are open by a hERG-specific voltage protocol, and the compound effects are directly characterized by their block of the hERG current. The assay is performed on an automated platform, Q-Patch. All compounds are tested by four-point dose response curves, and IC_{50} values (between 0.2 and 30 μM) are measured.[15]

In Vivo Pharmacokinetics Studies in Mice. NITD's Animal Care and Use Committee (IACUC), registered with Agri-Food and Veterinary Authority (AVA), Government of Singapore, approved all animal experimental protocols. Mice were allowed for acclimatization before initiation of pharmacokinetic (PK) experiments. Feed and water were given ad libitum.

Compounds **5**, **18**, **24**, **25**, **26**, **28**, **31**, and **32** were formulated at 3 mg/mL for a dose of 30 mg/kg given orally (po) and at 1 mg/mL for a dose of 5 mg/kg given intravenously (iv). Citrate buffer 100 mM, pH 3.5, was used to formulate compounds **5**, **18**, **24**, **25**, **26**, and **28** prior to po administration, while citrate buffer 50 mM, pH 4.5, was used for iv administration. Both were clear solutions. For compounds **31** and **32**, the solution formulation for both po and iv dosing was ethanol/PEG400/10% vitamin ETPGS (10:30:60). Blood samples were collected at 0.08, 0.25, 0.5, 1, 2, 4, 8, 16, and 24 h following po dosing. Sampling was identical following iv dosing except that the first time point was 0.02 h. Groups of three mice were used for each time point. Blood was centrifuged at 13 000 rpm for 7 min at 4 °C and plasma harvested and stored at −20 °C until analysis.

dx.doi.org/10.1021/jm2003359 |*J. Med. Chem.* 2011, 54, 5116–5130

PK studies for compounds **11** and **30** were conducted at GNF. In-life studies were carried out under protocols approved by the Animal Care and Use Committee (IACUC) of GNF. Compounds **11** and **30** were formulated at 2.5 mg/mL in 75% PEG300 and 25% D5W (5% dextrose in distilled water) solution and were filtered using a 0.45 μm syringe filter. The filtered solutions were dosed intravenously via the lateral tail vein at 5 mg/kg with a dosing volume of 2 mL/kg to male Balb/c mice (n = 3 per group). The filtered solutions were also administered orally at 20 mg/kg (with a dosing volume of 8 mL/kg) to another groups of mice (n = 3 per group). Six blood samples of 50 μL each were collected serially from each animal via retro-orbital sinus up to 24 h after dosing. Blood samples were collected into heparin microtainer and centrifuged, and the plasma was separated and frozen until analysis. Plasma samples were analyzed by LC/MS/MS.

Extraction and LC/MS Analysis. Plasma samples were extracted with acetonitrile/methanol/acetic acid (90:9.8:0.2) for analytes and internal standard (analogue from the same series) using a 8 to 1 extractant to plasma ratio. Analyte quantitation was performed by LC/MS/MS. Liquid chromatography was performed using an Agilent 1100 HPLC system (Santa Clara, CA), with the Agilent Zorbax XDB phenyl (3.5 μ, 4.6 mm × 75 mm) column at an oven temperature of 45 °C, coupled with a QTRAP4000 triple quadruple mass spectrometer (Applied Biosystems, Foster City, CA). Instrument control and data acquisition were performed using the Applied Biosystems software Analyst, version 1.4.2. The mobile phases used were (A) water−acetic acid (99.8:0.2, v/v) and (B) acetonitrile−acetic acid (99.8:0.2, v/v), using a gradient, with flow rate of 1.0 mL/min, and run time of 5 min. Compound detection on the mass spectrometer was performed in electrospray positive ionization mode and using multiple reaction monitoring (MRM) for specificity (transitions: compound **5** 384.2/101.2, compound **18** 384.3/101.2, compound **24** 412.3/327.2, compound **25** 380.4/118.2, compound **26** 408.5/280.3, compound **28** 428.2/343.2, compound **31** 418.3/101.4, compound **32** 446.3/361.2,) together with their optimized MS parameters. The lower limit of quantification ranged between 0.5 and 23 ng/mL for all the compounds studied.

For PK studies of compounds **11** and **30** in mice, plasma samples (20 μL) were extracted with a solution of acetonitrile/methanol (3:1) containing internal standard. The samples were vortexed, then centrifuged with an Eppendorf centrifuge 5810R (Eppendorf, Hamburg, Germany) at a setting of 4000 rpm for 10 min at room temperature. The supernatant was transferred to a clean 96-well analysis plate for LC/MS/MS analysis. An aliquot (10 μL) was injected onto a Phenomenex C18 guard column (4 mm × 2 mm) followed by a Zorbax SB-C8 analytical column (2.1 mm × 50 mm, 5 μm, Agilent Technologies Inc., Palo Alto, CA, U.S.). Separation was carried out using a gradient elution method with a mobile phase consisting of 0.05% formic acid in water (solvent A) and 0.05% formic acid in acetonitrile (solvent B). The flow rate was 600 μL/min. The HPLC system, consisting of Agilent 1100 series binary pump (Agilent Technologies Inc.), Agilent 1100 series microvacuum degasser (Agilent Technologies Inc.), HTC PAL CTC analytics autosampler (LEAP Technologies, Carborro, NC), and VICI two-position actuator (Valco Int., Huston, Texas, U.S.), was interfaced to a MDS SCIEX API-4000 triple quadruple mass spectrometer (MDS Inc., Toronto, Canada). Mass spectral analyses were carried out using electrospray source in the positive ion mode and using multiple reaction monitoring (MRM) for quantification. MRM transitions of 412.2/327.2 and 430.1/304.0 were used for compounds **11** and **30**, respectively.

Pharmacokinetic Analysis. The mean value from the three animals at each time point was plotted against time to give plasma concentration−time profile. Pharmacokinetic parameters were determined using Watson LIMS, version 7.2 (Thermo Electron Corporation, PA, U.S.), by noncompartmental analysis. Pharmacokinetic parameters for compounds **11** and **30** were calculated by noncompartmental regression analysis using an in-house fitting program developed at GNF. The oral bioavailability (F) was calculated as the ratio between the area under the curve (AUC) following oral administration and the AUC following intravenous administration corrected for dose (F = $[(AUC_{po})(dose_{iv})]/[(AUC_{iv})(dose_{po})]$.

In Vivo Antimalarial Activity. All in vivo efficacy studies were approved by the veterinary authorities of the Canton Basel-Stadt. In vivo antimalarial activity was usually assessed for groups of three female NMRI mice (20−22 g) intravenously infected on day zero with 2×10^7 erythrocytes parasitized with *P. berghei* GFP ANKA malaria strain (PbGFPCON donation from AP Waters and CJ Janse, Leiden University, The Netherlands).[10a,16] Untreated control mice die typically between day 6 and day 7 after infection. Experimental compounds were formulated in 7% Tween 80/3% ethanol or 75% PEG300/25% D5W as indicated. Compounds were administered orally in a volume of 10 mL/kg either as a single dose (24 h post infection) or as three consecutive daily doses (24, 48, and 72 h after infection). With the single dose regimen parasitemia was determined (72 h after infection). For the triple dose regimen (96 h after infection), standard flow cytometry techniques were used.[16] Activity was calculated as the difference between the mean percent parasitemia for the control and treated groups expressed as a percentage of the control group. The survival time in days was also recorded up to 30 days after infection. A compound was considered curative if the animal survived to day 30 after infection with no detectable parasites.

Chemistry. Unless otherwise noted, materials were obtained from commercial suppliers and were used without purification. Removal of solvent under reduced pressure refers to distillation using Büchi rotary evaporator attached to a vacuum pump (∼3 mmHg). Products obtained as solids or high boiling oils were dried under vacuum (∼1 mmHg).

Purification of compounds by high pressure liquid chromatography was achieved using a Waters autopurification system consisting of a 2767 autosampler/fraction collector, a 2525 binary gradient module, a 2487 UV detector, and a ZQ mass spectrometer. Compounds were purified using flow rate of 30 mL/min with a 50 mm × 20 mm i.d. Ultra 120 5 μm C18Q column (Peeke Scientific, Novato, CA). A 7.5 min linear gradient from 10% solvent A (acetonitrile with 0.035% trifluoroacetic acid) in solvent B (water with 0.05% trifluoroacetic acid) to 90% A was used, followed by a 2.5 min hold at 90% A. ^{1}H NMR spectra were recorded on Bruker XWIN-NMR (400 or 600 MHz) spectrometer. Proton resonances are reported in parts per million (ppm) downfield from tetramethylsilane (TMS). ^{1}H NMR data are reported as multiplicity (s, singlet; d, doublet; t, triplet; q, quartet; quint, quintuplet; sept septuplet; dd, doublet of doublets; dt, doublet of triplets; bs, broad singlet), number of protons, and coupling constant in hertz. For spectra obtained in $CDCl_3$, DMSO-d_6, CD_3OD, the residual protons (7.27, 2.50, and 3.31 ppm, respectively) were used as the reference.

Analytical thin-layer chromatography (TLC) was performed on commercial silica plates (Merck 60-F 254, 0.25 mm thickness). Compounds were visualized by UV light (254 nm). Flash chromatography was performed either by CombiFlash (separation system Sg. 100c, ISCO) or using silica gel (Merck Kieselgel 60, 230−400 mesh). Elemental analyses were carried out by Midwest Microlabs LLC, Indianapolis, IN.

Purity of Compounds. All compounds were analyzed with a Waters ZQ 2000 LC/MS system, which used an Agilent binary pump and photodiode array detector (PDA) along with a Sedere 75 evaporative light scattering detector (ELSD). Samples were injected from 96-well or 384-well plates with a Leap Technologies HTS Pal autosampler. The mobile phases used were (A) H_2O + 0.05% TFA and (B) ACN + 0.035% TFA. A gradient HPLC method with flow of 1.0 mL/min started at 5% B, with a hold of 0.1 min before a linear increase to 95% B at 2.70 min. At 2.71 min the B mobile phase was increased to 100% and held until 2.98 min. Total run time was 3.0 min. The column used was a Waters Atlantis dC18 2.1 mm × 30 mm, 3 μm. The mass spectrometer was operated in positive mode, with a spray voltage of 3.2 kV and cone voltage of 30 V. The source

and desolvation temperatures were 130 and 400 °C, respectively, with 600 L/h of nitrogen desolvation flow. The progress of reactions and the purity of products were measured using 254 and 220 nm wavelengths and electrospray ionization (ESI) positive mode. Mass spectra were obtained in ESI positive mode. All the reported compounds were found to be >95% when analyzed at the 254 nm wavelength.

Compound 1a: 2-Amino-1-(3-(benzo[*d*][1,3]dioxol-5-ylamino)-2-phenyl-5,6-dihydroimidazo[1,2-*a*]pyrazin-7(8*H*)-yl)-ethanone. The structure of **1a** is as follows:

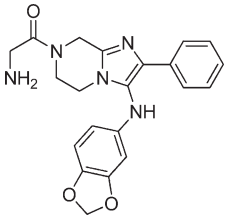

Synthesis of 1-2: *N*-(Benzo[*d*][1,3]dioxol-5-yl)-2-phenyl-5,6,7,8-tetrahydroimidazo[1,2-*a*]pyrazin-3-amine

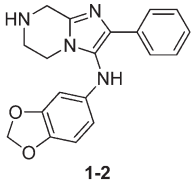

1-2

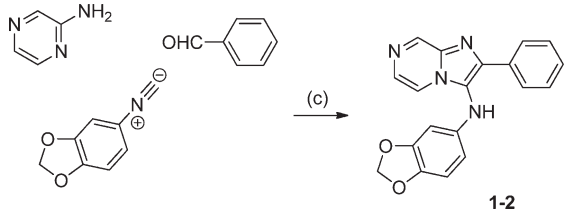

1-2

To a stirred solution of isocyanide (158 mg, 1.66 mmol) in 10 mL of MeOH were added benzaldehyde (0.25 mL, 2.49 mmol) and 2-aminopyrazine (281 mg, 1.91 mmol), followed by 1.0 N $HClO_4$ in MeOH (0.17 mL, 0.17 mmol). The reaction mixture was stirred at room temperature for 3 h. The reaction mixture was directly taken to mass-triggered HPLC purification. The collected MeCN/water solution was concentrated and dried on a lyophilizer to give 296 mg of compound **1-2** as a powdery product. ^{1}H NMR ($CDCl_3$, 400 MHz) δ 9.23 (d, J = 1.2 Hz, 1H), 8.03 (d, J = 4.8 Hz, 1H), 7.91−7.94 (m, 3H), 7.26−7.44 (m, 3H), 6.68 (d, J = 8.4 Hz, 1H), 6.32 (br, 1H), 6.25 (d, J = 2.4 Hz, 1H), 6.00 (dd, J = 8.4, 2.4 Hz, 1H), 5.93 (s, 2H).

Synthesis of 1-3: *N*-(Benzo[*d*][1,3]dioxol-5-yl)-2-phenyl-5,6,7,8-tetrahydroimidazo[1,2-*a*]pyrazin-3-amine

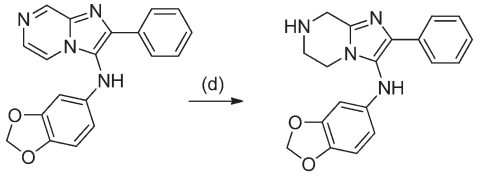

1-2 **1-3**

To a stirred solution of compound **1-2** (181 mg, 0.54 mmol) in 10 mL of MeOH was added Pd/C (58 mg, 0.054 mmol). The reaction mixture was evacuated and back-filled with H_2. The reaction mixture was stirred at room temperature overnight. The solid was filtered off, and solvent was removed. The 400 MHz proton NMR of the crude product proved it to be **1-3**. ^{1}H NMR (MeOH-d_4, 400 MHz) δ 7.72−7.4 (m, 2H), 7.38−7.33 (m, 3H), 6.66 (d,, J = 8.29 Hz, 1H), 6.33 (d, J = 2.32 Hz, 1H), 6.14 (dd, J = 8.3, 2.3 Hz, 1H), 5.86 (s, 2H), 4.57 (s, 2H), 4.08 (t, J = 5.7 Hz, 2H), 3.68 (t, J = 5.7 Hz, 2H).

Synthesis of Compound 1a: 2-Amino-1-(3-(benzo[*d*][1,3]dioxol-5-ylamino)-2-phenyl-5,6-dihydroimidazo[1,2-*a*]pyrazin-7(8*H*)-yl)ethanone. To a stirred solution of *N*-BOC-glycine (142 mg, 0.81 mmol) in 2 mL of DMF were added HATU (308 mg, 0.81 mmol) and DIEA (0.28 mL, 1.62 mmol). After the mixture was stirred for 10 min, compound **1-3** (180 mg, 0.54 mmol) was added. The reaction mixture was stirred at room temperature for 3 h. Solvent was removed, and the crude product was subjected to MS-triggered HPLC purification. The collected MeCN/water solution was concentrated until no more MeCN was left. The remaining aqueous solution was neutralized with $NaHCO_3$ and extracted with DCM. The organic solution was dried and concentrated. The residue was dissolved in 1:1 MeCN/water solvent and dried on a lyophilizer to give 192 mg of powdery amide coupled product.

A solution of the above obtained amide (265 mg, 0.54 mmol) in 10 mL of 4:1 DCM and TFA was stirred at room temperature for 2 h. Solvent was removed, and the crude product was subjected to MS-triggered HPLC separation. The collected MeCN/water solution was concentrated until no more MeCN was left. The remaining aqueous solution was neutralized with $NaHCO_3$ and extracted with DCM. The organic solution was dried and concentrated. The oil was then dissolved in 1:1 MeCN/water solvent and dried on a lyophilizer to give a powdery product in quantitative yield. ^{1}H NMR (400 MHz, MeOH-d_4) δ 7.75 (m, 2H), 7.19 (m, 2H), 7.18 (m, 1H), 6.61 (m, 1H), 6.22 (m, 1H), 6.03 (m, 1H), 5.82 (m, 2H), 4.75 (m, 2H), 3.78−4.05 (m, 6H). M/Z = 392.2 (M + 1).

Compound 1b: 2-Amino-1-(3-(benzo[*d*][1,3]dioxol-5-ylamino)-2-phenyl-5,6-dihydroimidazo[1,2-*a*]pyrazin-7(8*H*)-yl)-3-phenylpropan-1-one

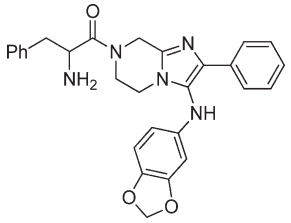

Compound **1b** was synthesized from compound **1-3** by a HATU mediated coupling with 2-(*tert*-butoxycarbonylamino)-3-phenylpropanoic acid followed by TFA mediated deprotection. ^{1}H NMR (400 MHz, MeOH-d_4) δ 7.67 (m, 2H), 7.37−7.20 (m, 8H), 6.65 (m, 1H), 6.25 (m, 1H), 6.07 (td, J = 2.29 Hz, J = 8.14 Hz, 1H), 5.85 (m, 2H), 4.79 (dd, J =5.86 Hz, J = 9.79 Hz, 1H), 4.59−4.19 (m, 2H), 3.57−3.83 (m, 3H), 3.16−2.93 (m, 3H). M/Z = 482.3 (M + 1).

Compound 1c: 2-Amino-1-(3-(benzo[*d*][1,3]dioxol-5-ylamino)-2-phenyl-5,6-dihydroimidazo[1,2-*a*]pyrazin-7(8*H*)-yl)-4-methylpentan-1-one

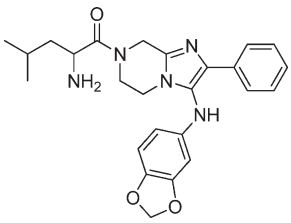

Compound **1c** was synthesized from compound **1-3** by a HATU mediated coupling with 2-((*tert*-butoxycarbonyl)amino)-4-methylpentanoic acid

dx.doi.org/10.1021/jm2003359 |*J. Med. Chem.* 2011, 54, 5116–5130

followed by TFA mediated deprotection. ^{1}H NMR (400 MHz, MeOH-d_4) δ 7.78 (m, 2H), 7.42 (m, 3H), 6.66 (m, 1H), 6.36 (m, 1H), 6.13 (m, 1H), 5.85 (m, 2H), 5.24 (m, 1H), 4.58 (m, 1H), 4.05 (m, 4H), 3.35 (s, 2H), 1.76 (m, 2H), 1.03 (m, 6H). M/Z = 448.2 (M + 1).

Compound 2: *N*,2-Bis(4-fluorophenyl)imidazo[1,2-*a*]pyrazin-3-amine

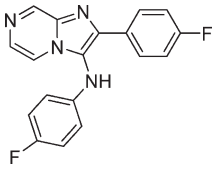

Compound **2** was synthesized by the following way: To a stirred solution of 2-aminopyrazine (683 mg, 7.18 mmol) in 50 mL of MeOH were added 4-fluorobenzaldehyde (1.16 mL, 10.8 mmol) and 1-fluoro-4-isocyanobenzene (1.0 g, 8.25 mmol), followed by 1.0 N $HClO_4$ in MeOH (0.72 mL, 0.72 mmol). The reaction mixture was stirred at room temperature overnight. The reaction mixture was concentrated, and the residue was subjected to flash chromatography purification. The collected organic solution was concentrated to give the compound **2** (1.1 g, 48%) as a yellow oil. ^{1}H NMR (400 MHz, MeOH-d_4) δ 8.96 (s, 1H), 7.95 (m, 3H), 7.82 (s, 1H), 7.07 (t, J = 8.84 Hz, 2H), 6.82 (t, J = 8.77 Hz, 2H),6.45 (m, 2H). M/Z = 323.3 (M + 1).

Compound 3: *N*,2-Bis(4-fluorophenyl)-5,6,7,8-tetrahydroimidazo[1,2-*a*]pyrazin-3-amine

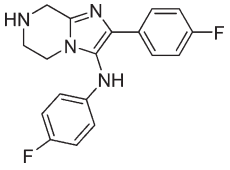

Compound **3** was synthesized by the following way: To a stirred solution of compound **2** (761 mg, 2.36 mmol) in 10 mL of MeOH was added Pd/C (258 mg, 0.24 mmol). The reaction mixture was evacuated and back-filled with H_2. The reaction mixture was stirred at room temperature overnight. The solid was filtered off, and solvent was removed. The product was subjected to mass-triggered HPLC purification. The obtained MeCN/water solution was combined and concentrated to give the final product as a yellow oil after neutralization (quantitative yield). ^{1}H NMR (300 MHz, DMSO-d_6) δ 7.81−7.72 (m, 2H), 7.11 (m, 2H), 6.97 (m, 2H), 6.56−6.52 (m, 2H), 3.86 (s, 2H), 3.55 (m, 2H), 3.02 (m, 2H). M/Z = 327.2 (M + 1).

Compound 5: 2-Amino-1-(2-(4-fluorophenyl)-3-(4-fluorophenylamino)-5,6-dihydroimidazo[1,2-*a*]pyrazin-7(8*H*)-yl)-ethanone

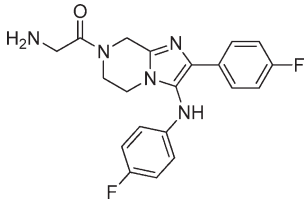

Compound **5** was synthesized from compound **3** by a HATU mediated coupling with *N*-BOC-glycine followed by TFA mediated deprotection (72% isolated yield) using a protocol for synthesis of compound **1a**. ^{1}H NMR (400 MHz, MeOH-d_4) δ 7.59−7.56 (m, 2H), 7.12 (t, J = 8.8 Hz, 2H), 6.86 (t, J = 8.8 Hz, 2H), 6.68−6.65 (m, 2H), 5.04−5.00 (m, 2H), 4.08−3.92 (m, 6H). M/Z = 384.2 (M + 1). Elemental analysis (compound + 3HCl): % C, 48.75; % H, 4.50; % N, 14.21 (calculated). % C = 48.86/48.58; % N = 14.11/13.95; % H = 4.69/4.49 (experimental).

Compound 6: *N*-(tert-butyl)-2-(4-fluorophenyl)imidazo[1,2-*a*]pyrazin-3-amine

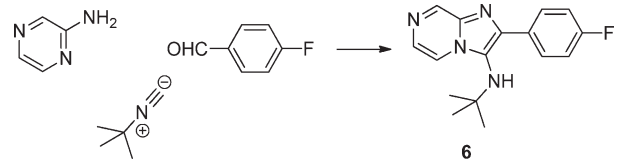

6

To a stirred solution of 2-aminopyrazine (571 mg, 6.0 mmol) in 10 mL of MeOH were added 4-fluorobenzaldehyde (0.97 mL, 9.0 mmol), 2-isocyano-2-methylpropane (0.78 mL, 6.9 mmol), and 1.0 N $HClO_4$ in MeOH (0.60 mL, 0.60 mmol). The reaction mixture was stirred at room temperature for 3 h. Solvent was removed and the residue was subjected to flash chromatography purification to give compound **6** as white solid. ^{1}H NMR ($CDCl_3$, 400 MHz) δ 8.97 (d, J = 1.6 Hz, 1H), 8.10 (dd, J = 1.6, 4.4 Hz, 1H), 7.90−7.94 (m, 2H), 7.86 (d, J = 4.66 Hz, 1H), 7.13 (t, J = 8.8 Hz, 2H), 1.04 (s, 9H).

Compound 7: 2-(4-fluorophenyl)imidazo[1,2-*a*]pyrazin-3-amine

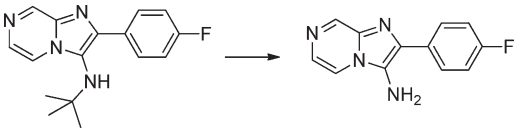

6 7

A solution of compound **6** (284 mg, 1.0 mmol) in 10 mL of 4:1 DCM and TFA was stirred at room temperature for 2 h. Solvent was removed, and the product was directly used in the next step after neutralization. ^{1}H NMR (300 Hz, $CDCl_3$) δ 8.82 (s, 1H), 8.28 (d, J = 4.8 Hz, 1H), 8.05−8.09 (m, 2H), 7.76 (d, J = 4.5 Hz, 1H), 7.27−7.33 (m, 2H), 5.79 (s, 2H). M/Z = 229 (M + 1).

Compound 8: 3-Amino-1-(2-(4-fluorophenyl)-3-(4-fluorophenylamino)-5,6-dihydroimidazo[1,2-*a*]pyrazin-7(8*H*)-yl)-propan-1-one

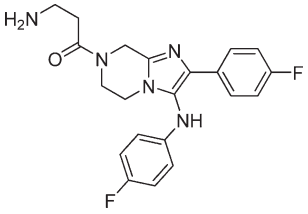

Compound **8** was synthesized from compound **3** by a HATU mediated coupling with 3-(*tert*-butoxycarbonylamino)propanoic acid followed by TFA mediated deprotection. ^{1}H NMR (CD_3OD, 400 MHz) δ 7.61−7.65 (m, 2H), 6.87−6.92 (m, 2H), 6.75−6.80 (m, 2H), 6.45−6.49 (m, 2H), 4.71 (d, J = 4.0 Hz, 2H), 3.82−3.90 (m, 2H), 3.62−3.74 (m, 2H), 2.81−2.84 (m, 2H), 2.51−2.57 (m, 2H). M/Z = 398.4 (M + 1).

Compound 9: (*S*)-2-Amino-1-(2-(4-fluorophenyl)-3-(4-fluorophenylamino)-5,6-dihydroimidazo[1,2-*a*]pyrazin-7(8*H*)-yl)-propan-1-one

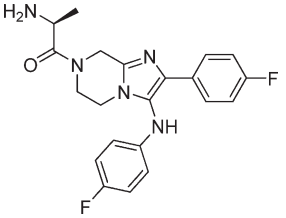

Compound **9** was synthesized from compound **3** by a HATU mediated coupling with (*S*)-2-(*tert*-butoxycarbonylamino)propanoic acid followed by

dx.doi.org/10.1021/jm2003359 |*J. Med. Chem.* 2011, 54, 5116–5130

TFA mediated deprotection. ^{1}H NMR (CD_3OD, 400 MHz) δ 7.63 (m, 2H), 6.95 (m, 2H), 6.82 (m, 2H), 6.50 (m, 2H), 4.41 (m, 1H), 3.92−3.74 (m, 6H), 1.42 (d, J = 6.95 Hz, 3H). M/Z = 398.2 (M + 1).

Compound 10: (*S*)-2-Amino-1-(2-(4-fluorophenyl)-3-(4-fluorophenylamino)-5,6-dihydroimidazo[1,2-*a*]pyrazin-7(8*H*)-yl)-3-methylbutan-1-one

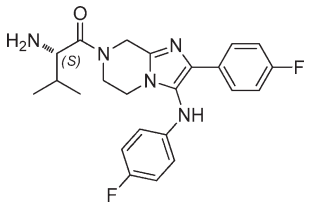

Compound **10** was prepared from compound **3** by a HATU mediated coupling reaction with (*S*)-2-(*tert*-butoxycarbonylamino)-3-methylbutanoic acid followed by a TFA mediated deprotection. ^{1}H NMR (DMSO-d_6, 400 MHz) δ 8.15 (bs, 1H), 8.02 (s, 1H), 7.77 (m, 2H), 7.19 (m, 2H), 7.00 (m, 2H), 6.61 (m, 2H), 5.05−4.87 (m, 1H), 4.69−4.41 (m, 1H), 4.23−4.11 (m, 1H), 3.98−3.77 (m, 1H), 3.00 (m, 1H), 2.51 (s, 2H), 2.1 (m, 1H), 0.95 (dd, J = 22, 6.72 Hz, 6H). M/Z = 426 (M + 1)

Compound 11: 2-Amino-1-(2-(4-fluorophenyl)-3-(4-fluorophenylamino)-5,6-dihydroimidazo[1,2-*a*]pyrazin-7(8*H*)-yl)-2-methylpropan-1-one

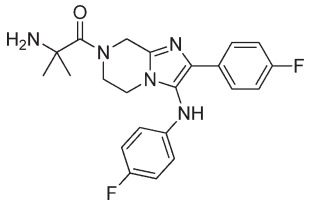

Compound **11** was synthesized from compound **3** by a HATU mediated coupling with 2-(*tert*-butoxycarbonylamino)-2-methylpropanoic acid followed by TFA mediated deprotection. ^{1}H NMR (MeOH-d_4, 400 Hz) δ7.70−7.67 (m, 2H), 7.22 (t, J = 8.8 Hz, 2H), 6.97(t, J = 8.8 Hz,2H), 6.8−6.77 (m, 2H), 5.16 (s, 2H), 4.24 (m, 2H), 4.07 (m, 2H), 1.76 (s, 6H). M/Z = 412.2 (M + 1). Elemental analysis of HCl salt (compound + 2HCl + 0.50 H_2O): % C, 53.56; % H, 5.31; % N, 14.19 (calculated). % C = 53.98/53.69; % N = 14.07/13.97; % H = 5.16/4.98 (experimental).

Compound 12: (*S*)-2-Amino-1-(2-(4-fluorophenyl)-3-(4-fluorophenylamino)-5,6-dihydroimidazo[1,2-*a*]pyrazin-7(8*H*)-yl)-3-phenylpropan-1-one

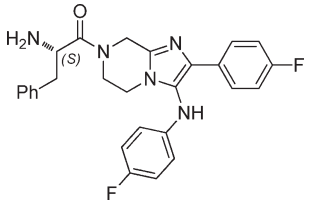

Compound **12** was synthesized from compound **3** by a HATU mediated coupling with (*S*)-2-(*tert*-butoxycarbonylamino)-3-phenylpropanoic acid followed by TFA mediated deprotection. ^{1}H NMR ($CDCl_3$, 400 Hz) δ 9.06 (bs), 7.94 (bs), 7.3−6.93 (m, 11H), 6.55 (m, 2H), 5.5−4.62 (m, 2H), 4.28 (m, 1H), 3.68−2.60 (m, 6H). M/Z = 474.4 (M + 1).

Compound 13: (*R*)-2-Amino-1-(2-(4-fluorophenyl)-3-(4-fluorophenylamino)-5,6-dihydroimidazo[1,2-*a*]pyrazin-7(8*H*)-yl)-3-phenylpropan-1-one

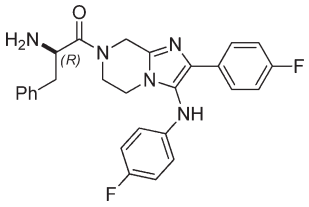

Compound **13** was synthesized from compound **3** by a HATU mediated coupling with (*R*)-2-(*tert*-butoxycarbonylamino)-3-phenylpropanoic acid followed by TFA mediated deprotection. ^{1}H NMR (400 MHz, MeOH-d_4) δ 7.65 (m, 1H), 7.18 (m, 8H), 6.96 (m, 2H), 6.82 (m, 1H), 6.49 (m, 1H), 4.65−4.8 (m, 2H), 4.00−4.49 (m, 2H), 3.38−3.57 (m, 3H), 2.73−3.00 (m, 2H). M/Z = 474.4 (M + 1).

Compound 14: 2-Amino-1-(3-((4-fluorophenyl)amino)-2-phenyl-5,6-dihydroimidazo[1,2-*a*]pyrazin-7(8*H*)-yl)-2-methylpropan-1-one

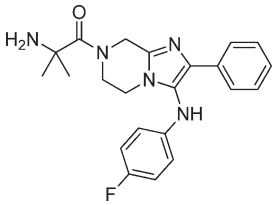

Compound **14** was synthesized following the same sequence as compound **1** involving an Ugi reaction, reduction using palladium on carbon followed by HATU mediated coupling with *N*-BOC-dimethylglycine and TFA mediated deprotection. ^{1}H NMR (DMSO-d_6, 400 MHz) δ 8.25 (bs, 1H), 8.01 (s, 1H), 7.73 (m, 2H), 7.35 (m, 2H), 7.25 (m, 1H), 7.00 (t, J = 8.04 Hz, 2H), 6.62 (m, 2H), 4.40 (m, 2H), 4.08 (m, 2H), 3.76 (m, 2H), 1.60 (s, 6H). M/Z = 394.4 (M + 1).

Compound 15: 2-Amino-1-(2-(4-chlorophenyl)-3-((4-fluorophenyl)amino)-5,6-dihydroimidazo[1,2-*a*]pyrazin-7(8*H*)-yl)-ethanone

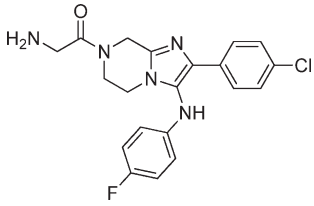

Compound **15** was synthesized following the same sequence as compound **1** involving an Ugi reaction, reduction using palladium on carbon followed by HATU mediated coupling with *N*-BOC-glycine and TFA mediated deprotection. ^{1}H NMR (400 MHz, MeOH-d_4) δ 7.68 (m, 2H), 7.38 (m, 2H), 6.94 (m, 2H), 6.69 (m, 2H), 5.05−5.00 (m, 2H), 4.12 (s, 2H), 3.83−3.99 (m, 4H). M/Z = 400.2 (M + 1).

dx.doi.org/10.1021/jm2003359 |*J. Med. Chem.* 2011, 54, 5116–5130

Compound 16: 2-Amino-1-(3-((4-fluorophenyl)amino)-2-(4-methoxyphenyl)-5,6-dihydroimidazo[1,2-*a*]pyrazin-7(8*H*)-yl)ethanone

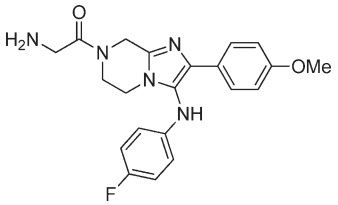

Compound **16** was synthesized following the same sequence as compound **1** involving an Ugi reaction, reduction using palladium on carbon followed by HATU mediated coupling with *N*-Boc-glycine and TFA mediated deprotection. ^{1}H NMR (400 MHz, MeOH-d_4) δ 7.58 (d, J = 8.79 Hz, 2H), 6.98 (m, 4H), 6.75 (m, 2H), 5.07−5.00 (m, 2H), 4.14 (s, 2H), 4.02 (m, 4H), 3.18 (s, 3H). M/Z = 396.2 (M + 1).

Compound 17: 2-Amino-1-(3-((4-fluorophenyl)amino)-2-(*p*-tolyl)-5,6-dihydroimidazo[1,2-*a*]pyrazin-7(8*H*)-yl)ethanone

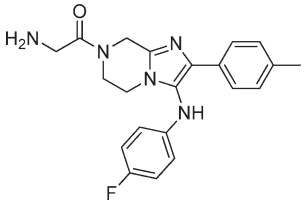

Compound **17** was synthesized following the same sequence as compound **1** involving an Ugi reaction, reduction using palladium on carbon followed by HATU mediated coupling with *N*-Boc-glycine and TFA mediated deprotection. ^{1}H NMR (400 MHz, MeOH-d_4) δ 7.53 (d, J = 8.12 Hz, 2H), 7.17 (m, 2H), 6.94 (m, 2H), 6.72 (m, 2H), 5.07−5.00 (m, 2H), 4.13 (s, 2H), 4.02 (m, 4H), 2.35 (s, 3H). M/Z = 380.4 (M + 1).

Compound 18: 2-Amino-1-(3-((4-fluorophenyl)amino)-2-(3-fluorophenyl)-5,6-dihydroimidazo[1,2-*a*]pyrazin-7(8*H*)-yl)-ethanone

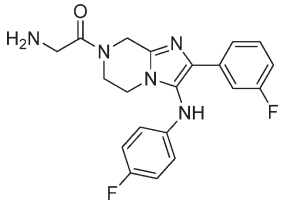

Compound **18** was synthesized following the same sequence as compound **1** involving an Ugi reaction, reduction using palladium on carbon followed by HATU mediated coupling with *N*-BOC-glycine and TFA mediated deprotection. ^{1}H NMR (MeOH-d_4, 400 Hz) δ 7.55−7.53 (m, 1H), 7.47−7.45 (m, 2H), 7.15 (m, 1H), 6.96−6.94 (m, 2H), 6.84−6.81 (m, 2H), 5.20 (m, 2H), 4.25−4.20 (m, 6H), 3.35 (s, NH). M/Z = 384.2 (M + 1).

Compound 19: 2-Amino-1-(2-(2-fluorophenyl)-3-((4-fluorophenyl)amino)-5,6-dihydroimidazo[1,2-*a*]pyrazin-7(8*H*)-yl)-2-methylpropan-1-one

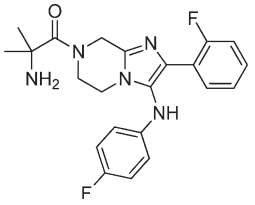

Compound **19** was synthesized following the same sequence as compound **1** involving an Ugi reaction, reduction using palladium on carbon followed by HATU mediated coupling with *N*-BOC-dimethylglycine and TFA mediated deprotection. ^{1}H NMR (MeOH-d_4, 400 Hz) δ 7.41 (m, 1H), 7.28 (m, 1H), 7.08 (m, 2H), 6.79 (m, 2H), 6.56 (m, 2H), 4.93(m, 2H), 4.00 (m, 2H), 3.86 (t, J = 5.17 Hz, 2H), 1.64 (s, 6H). M/Z = 412.2 (M + 1).

Compound 20: 2-Amino-1-(2-(3,4-difluorophenyl)-3-(*p*-tolylamino)-5,6-dihydroimidazo[1,2-*a*]pyrazin-7(8*H*)-yl)-2-methylpropan-1-one

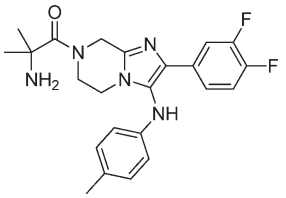

Compound **20** was synthesized following the same sequence as compound **1** involving an Ugi reaction, reduction using palladium on carbon followed by HATU mediated coupling with *N*-BOC-dimethylglycine and TFA mediated deprotection. ^{1}H NMR (MeOH-d_4, 400 Hz) δ 7.53−7.48 (m, 1H), 7.44−7.41 (m, 1H), 7.17 (m, 1H), 6.9 (m, 2H), 6.48 (m, 2H), 4.88 (m, 2H), 4.05 (m, 2H), 3.81 (m, 2H), 2.12 (s, 3H), 1.62 (s, 6H). M/Z = 426.2(M + 1).

Compound 21: 2-Amino-1-(3-(cyclohexylamino)-2-(4-fluorophenyl)-5,6-dihydroimidazo[1,2-*a*]pyrazin-7(8*H*)-yl)-2-methylpropan-1-one

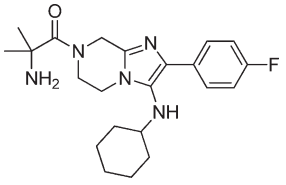

Compound **21** was synthesized following the same sequence as compound **1** involving an Ugi reaction, reduction using palladium on carbon followed by HATU mediated coupling with *N*-BOC-dimethylglycine and TFA mediated deprotection. ^{1}H NMR (MeOH-d_4, 400 Hz) δ 7.66 (m, 2H), 7.18 (t, J = 8.74 Hz, 2H), 4.95 (m, 2H), 4.13 (m, 2H), 4.11 (m, 2H), 2.74 (m, 1H), 1.73 (m, 2H), 1.68 (s, 6H), 1.37−1.60 (m, 4H), 1.05−1.15 (m, 4H). M/Z = 400.3 (M + 1).

Compound 22: 2-Amino-1-(2-(4-fluorophenyl)-3-(pyridin-3-ylamino)-5,6-dihydroimidazo[1,2-*a*]pyrazin-7(8*H*)-yl)-2-methylpropan-1-one

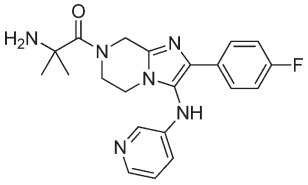

Compound **22** was synthesized following the same sequence as compound **1** involving an Ugi reaction, reduction using palladium on carbon followed by HATU mediated coupling with *N*-BOC-dimethylglycine and TFA mediated deprotection. ^{1}H NMR (400 MHz, MeOH-d_4) δ 8.15 (m, 1H), 7.7 (m, 3H), 7.57 (m, 2H), 7.1 (t, J = 8.74 Hz, 2H); 4.93 (m, 2H); 4.18 (s, 2H), 3.97 (m, 2H); 1.68 (s, 6H). M/Z = 395.4 (M + 1).

Compound 23: 2-Amino-1-(2-(4-fluorophenyl)-3-(3-fluorophenylamino)-5,6-dihydroimidazo[1,2-*a*]pyrazin-7(8*H*)-yl)-ethanone. The structure of **23** is as follows:

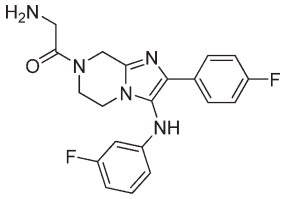

Synthesis of 23-3: *N*-(3-Fluorophenyl)-2-(4-fluorophenyl)-5,6,7,8-tetrahydroimidazo[1,2-*a*] pyrazin-3-amine

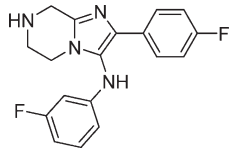

To a solution of compound **7** (69 mg, 0.30 mmol) in 6 mL of dioxane were added 1-bromo-3-fluorobenzene (66 μL, 0.60 mmol), $Pd_2(dba)_3$ (8 mg, 0.009 mmol), Xantphos (11 mg, 0.018 mmol), and Cs_2CO_3 (196 mg, 0.60 mmol) at room temperature. The reaction mixture was degassed and stirred at 120 °C under N_2 for 5 h. The reaction mixture was cooled to room temperature, and solid was filtered off. The resulting filtrate was concentrated. The residue was subjected to mass-triggered HPLC purification to give a yellow oil (64 mg, 66%) after neutralization. To a stirred solution of the obtained adduct (64 mg, 0.20 mmol) in 5 mL of MeOH was added Pd/C (21 mg, 0.02 mmol). The reaction mixture was evacuated and back-filled with H_2. The reaction mixture was stirred at room temperature overnight. The solid was filtered off, and solvent was removed. The residue was subjected to mass-triggered HPLC purification to give a yellow solid (42 mg, 66%).

Synthesis of 23: 2-Amino-1-(2-(4-fluorophenyl)-3-(3-fluorophenylamino)-5,6-dihydroimidazo[1,2-*a*]pyrazin-7(8*H*)-yl)-ethanone

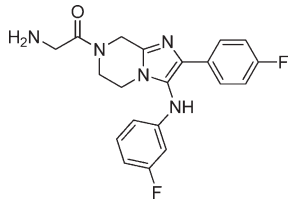

Compound **23** was synthesized from compound **23-3** by a HATU mediated coupling with *N*-Boc-glycine followed by TFA mediated deprotection. ^{1}H NMR (DMSO-d_6, 400 MHz) δ 8.24 (bs, 1H), 8.12 (s, 2H), 7.76 (m, 2H), 7.19 (m, 3H), 6.48 (m, 2H), 6.36 (m, 1H), 4.80 (m, 2H), 4.04−3.69 (m, 6H). M/Z = 384.4 (M + 1).

Compound 24: 2-Amino-1-(2-(3-fluorophenyl)-3-(4-fluorophenylamino)-5,6-dihydroimidazo[1,2-*a*]pyrazin-7(8*H*)-yl)-2-methylpropan-1-one

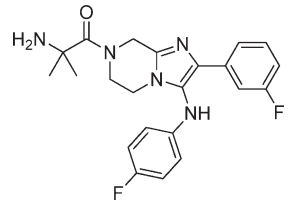

Compound **24** was synthesized from compound **23-3** by a HATU mediated coupling with 3-(*tert*-butoxycarbonylamino)propanoic acid followed by TFA mediated deprotection. ^{1}H NMR (MeOH-d_4, 400 Hz) δ 7.50−7.48 (m, 2H), 7.44−7.40 (m, 1H), 7.18 (m, 1H), 6.98 (t, J = 8.8 Hz, 2H), 6.82−6.79 (m, 2H), 5.18 (m, 2H), 4.25 (t, J = 4.8 Hz, 2H), 4.07 (t, J = 4.8 Hz, 2H), 1.76 (s, 6H). M/Z = 412.0 (M + 1). Elemental analysis of HCl salt (compound + 2HCl + 1.3H_2O): % C, 52.04; % H, 5.48; % N, 13.79 (calculated). % C = 51.95/52.02; % N = 13.37/13.5; % H = 5.26/5.32 (experimental).

Compound 25: 2-Amino-1-(2-(4-fluorophenyl)-3-(*p*-tolylamino)-5,6-dihydroimidazo[1,2-*a*]pyrazine-7(8*H*)-yl)-ethanone

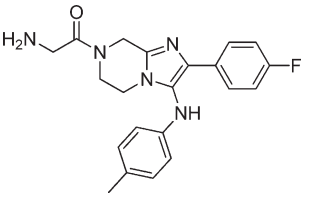

Compound **25** was synthesized following the same sequence as compound **1** involving an Ugi reaction, reduction using palladium on carbon followed by HATU mediated coupling with *N*-BOC-glycine and TFA mediated deprotection. ^{1}H NMR (400 MHz, MeOH-d_4) δ 7.74−7.71 (m, 2H), 7.21−7.17 (m, 2H), 7.03 (t, J = 8.0 Hz, 2H), 6.67 (d, J = 8.4 Hz, 2H), 5.17−5.15 (m, 2H), 4.22−3.98 (m, 6H), 2.22 (s, 3H). M/Z = 380.4 (M + 1). Elemental analysis of HCl salt (compound + 3HCl + 0.1H_2O): % C, 51.41; % H, 5.18; % N, 14.27 (calculated). % C = 51.75/51.52; % N = 14.34/14.29; % H = 5.17/5.15 (experimental).

Compound 26: 2-Amino-1-(2-(4-fluorophenyl)-3-(*p*-tolylamino)-5,6-dihydroimidazo[1,2-*a*]pyrazine-7(8*H*)-yl)-2-methylpropan-1-one

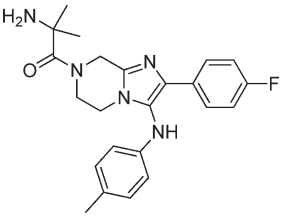

Compound **26** was synthesized following the same sequence as compound **1** involving an Ugi reaction, reduction using palladium on carbon followed by HATU mediated coupling with *N*-BOC-dimethylglycine and TFA mediated deprotection. ^{1}H-NMR (MeOH-d_4, 400 MHz) δ 7.72 (m, 2H), 7.18 (t, J = 8.0 Hz, 2H), 7.02 (m, 2H), 6.66 (d, J = 8.35 Hz, 2H), 5.19 (s, 2H), 4.28 (m, 2H), 4.07 (m, 2H), 2.21 (s, 3H), 1.77 (s, 6H). M/Z = 408.2 (M + 1). Elemental analysis of HCl salt (compound + 3HCl + 0.1H_2O): % C, 53.26; % H, 5.67; % N, 13.5 (calculated). % C = 53.28/53.18; % N = 13.39/13.32; % H = 5.92/5.81 (experimental).

Compound 27: 2-Amino-1-(3-(4-chlorophenylamino)-2-(4-fluorophenyl)-5,6-dihydroimidazo[1,2-*a*]pyrazin-7(8*H*)-yl)ethanone

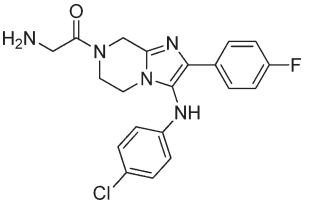

Compound **27** was synthesized from compound **7** using palladium catalyzed amination, reduction using palladium on carbon followed by

dx.doi.org/10.1021/jm2003359 |*J. Med. Chem.* 2011, 54, 5116–5130

HATU mediated coupling with *N*-BOC-glycine and TFA mediated deprotection. ^{1}H NMR (MeOH-d_4, 400 Hz) δ 7.59−7.56 (m, 2H), 7.15−7.09 (m, 4H), 6.68−6.65 (m, 2H), 5.05 (m, 2H), 4.04−3.87 (m, 6H). *M*/*Z* = 400.1 (M + 1).

Compound 28: 2-Amino-1-(3-(4-chlorophenylamino)-2-(4-fluorophenyl)-5,6-dihydroimidazo[1,2-*a*]pyrazin-7(8*H*)-yl)-2-methylpropan-1-one

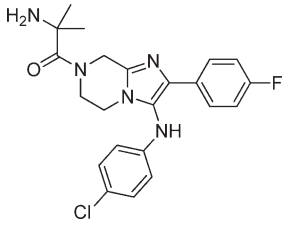

Compound **28** was synthesized from compound **7** using palladium catalyzed amination, reduction using palladium on carbon followed by HATU mediated coupling with *N*-BOC-dimethylglycine and TFA mediated deprotection. ^{1}H NMR (MeOH-d_4, 400 Hz) δ 7.70 (m, 2H), 7.21 (m, 4H), 6.8 (m, 2H), 5.19 (m, 2H), 4.26 (m, 2H), 4.0 (m, 2H), 1.77 (s, 6H). *M*/*Z* = 428.1 (M + 1). Elemental analysis of HCl salt (compound + 3HCl + H_2O): % C, 47.58; % H, 5.08, % N, 12.61 (calculated). % C = 47.46/47.57; % N = 12.48/12.5; % H = 4.72/4.81 (experimental).

Compound 29: 3-Amino-1-(2-(4-fluorophenyl)-3-(4-fluorophenylamino)-5,6-dihydroimidazo[1,2-*a*]pyrazin-7(8*H*)-yl)-propan-1-one

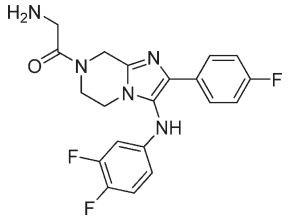

Compound **29** was synthesized from compound **7** using palladium catalyzed amination, reduction using palladium on carbon followed by HATU mediated coupling with *N*-BOC-glycine and TFA mediated deprotection. ^{1}H NMR (MeOH-d_4, 400 Hz) δ 7.64−7.59 (m, 2H), 6.96−6.89 (m, 3H), 6.38−6.34 (m, 1H), 6.27−6.23 (m, 1H), 4.74−4.63 (m, 2H), 3.94−3.41 (m, 6H). *M*/*Z* = 402.1 (M + 1).

Compound 30: 2-Amino-1-(3-(3,4-difluorophenylamino)-2-(4-fluorophenyl)-5,6-dihydroimidazo[1,2-*a*]pyrazin-7(8*H*)-yl)-2-methylpropan-1-one

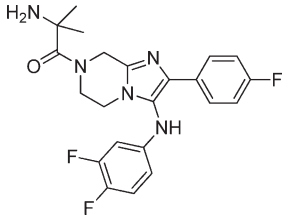

Compound **30** was synthesized following the same sequence as compound **1** involving an Ugi reaction, reduction using palladium on carbon followed by HATU mediated coupling with *N*-BOC-dimethylglycine and TFA mediated deprotection. ^{1}H NMR (400 MHz, MeOH-d_4) δ 7.64−7.70 (m, 2H), 6.95−6.91 (m, 3H), 6.33−6.39 (m, 1H), 6.27−6.22 (m, 1H), 4.97 (s, 2H), 4.17 (m, 2H), 3.73 (t, *J* = 2.8 Hz, 2H), 1.36 (s, 6H). *M*/*Z* = 430.2 (M + 1). Elemental analysis of HCl salt (compound + 2HCl + 0.40H_2O): % C, 51.85; % H, 4.91; % N, 13.74 (calculated). % C = 51.73/51.85; % N = 13.5/13.51; % H = 4.87/4.94 (experimental).

Compound 31: 2-Amino-1-(3-(4-chloro-3-fluorophenylamino)-2-(4-fluorophenyl)-5,6-dihydroimidazo[1,2-*a*]pyrazin-7(8*H*)-yl)ethanone

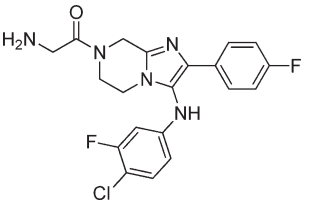

Compound **31** was synthesized from compound **7** using palladium catalyzed amination reduction using palladium on carbon followed by HATU coupling using *N*-Boc-glycine followed by TFA mediated deprotection. ^{1}H NMR (400 MHz, MeOH-d_4) δ 7.7 (m, 2H), 7.44−7.40 (m, 3H), 6.71 (m, 1H), 6.64 (m, 1H), 5.16 (s, 2H), 4.18−4.01 (m, 6H). *M*/*Z* = 418.0 (M + 1). Elemental analysis of HCl salt (compound + 2HCl + 2H_2O): % C, 45.6; % H, 4.59; % N, 13.29 (calculated). % C = 47.46/47.57; % N = 13.17/13.18; % H = 4.04/4.05 (experimental).

Compound 32: 2-Amino-1-(3-(4-chloro-3-fluorophenylamino)-2-(4-fluorophenyl)-5,6-dihydro imidazo[1,2-*a*]pyrazin-7(8*H*)-yl)-2-methylpropan-1-one

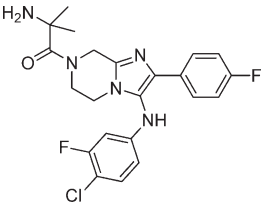

Compound **32** was synthesized from compound **7** using palladium catalyzed amination, reduction using palladium on carbon followed by HATU mediated coupling with *N*-BOC-dimethylglycine and TFA mediated deprotection. ^{1}H NMR (MeOH-d_4, 400 Hz) δ 7.59−7.56 (m, 2H), 7.2−7.11 (m, 3H), 6.6−6.57 (m, 2H), 5.04 (s, 2H), 4.14 (m, 2H), 3.97 (m, 2H), 1.69 (s, 6H). *M*/*Z* = 446.2 (M + 1). Elemental analysis (compound + 3HCl + 0.2H_2O): % C,47.28; % H, 4.58; % N, 12.53 (calculated). % C = 47.07/47.19; % N = 12.33/12.34; % H = 4.86/4.82 (experimental).

Compound 33: 2-Amino-1-(3-(2,4-difluorophenylamino)-2-(4-fluorophenyl)-5,6-dihydroimidazo[1,2-*a*]pyrazin-7(8*H*)-yl)-2-methylpropan-1-one

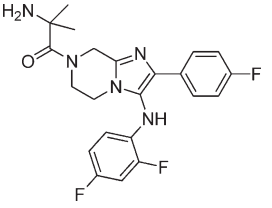

Compound **33** was synthesized from compound **7** using palladium catalyzed amination, reduction using palladium on carbon followed by HATU mediated coupling with *N*-BOC-dimethylglycine and TFA mediated deprotection. ^{1}H NMR (DMSO-d_6, 400 MHz) δ 8.24 (bs, 1H), 7.83 (bs, 1H), 7.75 (m, 2H), 7.25 (m, 1H), 7.17 (m, 2H), 6.81

dx.doi.org/10.1021/jm2003359 |*J. Med. Chem.* 2011, 54, 5116–5130

(m, 1H), 6.4 (m, 1H), 4.86 (m, 2H), 4.06 (m, 2H), 3.75 (m, 2H), 1.6 (m, 6H). M/Z = 430.2 (M + 1).

Compound 34: 2-Amino-1-(3-(3,5-difluorophenylamino)-2-(4-fluorophenyl)-5,6-dihydroimidazo[1,2-*a*]pyrazin-7(8*H*)-yl)-2-methylpropan-1-one

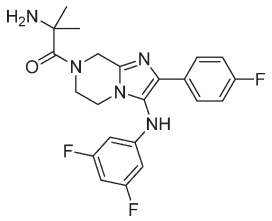

Compound **34** was synthesized from compound **7** using palladium catalyzed amination, reduction using palladium on carbon followed by HATU mediated coupling with *N*-BOC-dimethylglycine and TFA mediated deprotection. ^{1}H NMR (MeOH-d_4, 400 Hz) δ 7.6 (m, 2H), 7.08 (t, J = 8.76 Hz, 2H), 6.25 (m, 3H), 4.98 (s, 2H), 4.11 (t, J = 5.28 Hz, 2H), 3.9 (m, 2H), 1.66 (s, 6H). M/Z = 430.2 (M + 1).

AUTHOR INFORMATION

Corresponding Author

*Phone: +1 858-332-4751. E-mail: akc@gnf.org.

Author Contributions

#These authors made equal contribution to this work.

ACKNOWLEDGMENT

This work was supported by a joint grant to Genomics Institute of the Novartis Research Foundation, the Biomedical Primate Research Center, the Swiss Tropical and Public Health Institute, and the Novartis Institute for the Tropical Diseases from the U.K. Wellcome Trust and Medicines for Malaria Venture.

ABBREVIATIONS USED

ACT, artemisinin based combination therapy; WHO, World Health Organization; MMV, Medicines for Malaria Venture; GNF, Genomics Institute of the Novartis Research Foundation; C_{max}, the maximum plasma concentration; IC_{50}, half-maximal effective concentration; AUC, area under the concentration–time curve; hERG, human ether-a-go-go-related gene; PEG, polyethylene glycol; D5W, 5% dextrose in water

REFERENCES

(1) (a) World Health Organization. http://www.who.int/topics/malaria/en/ (accessed November 27, 2010). (b) *Annual Report 2009*; Medicines for Malaria Ventures (MMV): Geneva, Switzerland, 2009; http://www.mmv.org/sites/default/files/uploads/docs/publications/annual_report_2009_0.pdf. (c) Milner, E.; McCalmont, W.; Bhonsle, J.; Caridha, D.; Carroll, D.; Gardner, S.; Gerena, L.; Gettayacamin, M.; Lanteri, C.; Luong, T.; Melendez, V.; Moon, J.; Roncal, N.; Sousa, J.; Tungtaeng, A.; Wipf, P.; Dow, G. Structure–activity relationships amongst 4-position quinoline methanol antimalarials that inhibit the growth of drug sensitive and resistant strains of *Plasmodium falciparum*. *Bioorg. Med. Chem. Lett.* **2010**, *20* (4), 1347–1351. (d) Milner, E.; McCalmont, W.; Bhonsle, J.; Caridha, D.; Cobar, J.; Gardner, S.; Gerena, L.; Goodine, D.; Lanteri, C.; Melendez, V.; Roncal, N.; Sousa, J.; Wipf, P.; Dow, G. Anti-malarial activity of a non-piperidine library of next-generation quinoline methanols. *Malar. J.* **2010**, *9* (1), 51.

(2) (a) *Global Report on Antimalarial Drug Efficacy and Drug Resistance: 2000–2010*; World Health Organization: Geneva, Switzerland, 2010; http://whqlibdoc.who.int/publications/2010/9789241500470_eng.pdf. (b) A research agenda for malaria eradication: drugs. *PLoS Med.* **2011**, *8* (1), No. e1000402. (c) Sadanand, S. Malaria: an evaluation of the current state of research on pathogenesis and antimalarial drugs. *Yale J. Biol. Med.* **2010**, *83* (4), 185–191. (d) Wu, T.; Nagle, A. S.; Chatterjee, A. K. Road towards new antimalarials: overview of the strategies and their chemical progress. *Curr. Med. Chem.* **2011**, *18* (6), 853–871.

(3) Noedl, H.; Chanthap, L.; Se, Y.; Socheat, D.; Peou, S.; Schaecher, K.; Srivichai, S.; Teja-Isavadharm, P.; Smith, B.; Jongsakul, K.; Surasri, S.; Fukuda, M. Artemisinin resistance in Cambodia? *Trop. Med. Int. Health* **2007**, *12*, 69.

(4) (a) Deng, X. M.; Nagle, A.; Wu, T.; Sakata, T.; Henson, K.; Chen, Z.; Kuhen, K.; Plouffe, D.; Winzeler, E.; Adrian, F.; Tuntland, T.; Chang, J.; Simerson, S.; Howard, S.; Ek, J.; Isbell, J.; Tully, D. C.; Chatterjee, A. K.; Gray, N. S. Discovery of novel 1*H*-imidazol-2-yl-pyrimidine-4,6-diamines as potential antimalarials. *Bioorg. Med. Chem. Lett.* **2010**, *20* (14), 4027–4031.(b) Wu, T.; Nagle, A.; Sakata, T.; Deng, X. M.; Chen, Z.; Henson, K.; Chang, J.; Plouffe, D.; Tuntland, T.; Kuhen, K.; Winzeler, E.; Gray, N.; Chatterjee, A. K. Cell-Based Optimization of Novel Benzamides as Antimalarials. *Abstracts of Papers*, 236th National Meeting of the American Chemical Society, Philadelphia, PA, Aug 17–21, 2008; American Chemical Society: Washington, DC, 2008; MEDI 339, p 236. (c) Wu, T.; Nagle, A.; Sakata, T.; Henson, K.; Borboa, R.; Chen, Z.; Kuhen, K.; Plouffe, D.; Winzeler, E.; Adrian, F.; Tuntland, T.; Chang, J.; Simerson, S.; Howard, S.; Ek, J.; Isbell, J.; Deng, X.; Gray, N. S.; Tully, D. C.; Chatterjee, A. K. Cell-based optimization of novel benzamides as potential antimalarial leads. *Bioorg. Med. Chem. Lett.* **2009**, *19* (24), 6970–6974.

(5) Plouffe, D.; Brinker, A.; McNamara, C.; Henson, K.; Kato, N.; Kuhen, K.; Nagle, A.; Adrian, F.; Matzen, J. T.; Anderson, P.; Nam, T. G.; Gray, N. S.; Chatterjee, A.; Janes, J.; Yan, S. F.; Trager, R.; Caldwell, J. S.; Schultz, P. G.; Zhou, Y.; Winzeler, E. A. In silico activity profiling reveals the mechanism of action of antimalarials discovered in a high-throughput screen. *Proc. Natl. Acad. Sci. U.S.A.* **2008**, *105* (26), 9059–9064.

(6) Liu, B.; Chang, J.; Gordon, W. P.; Isbell, J.; Zhou, Y.; Tuntland, T. Snapshot PK: a rapid rodent in vivo preclinical screening approach. *Drug Discovery Today* **2008**, *13* (7–8), 360–367.

(7) (a) Varma, R. S.; Kumar, D. Microwave-accelerated three-component condensation reaction on clay: solvent-free synthesis of imidazo[1,2-*a*] annulated pyridines, pyrazines and pyrimidines. *Tetrahedron Lett.* **1999**, *40* (43), 7665–7669. (b) Bienayme, H.; Bouzid, K. A new heterocyclic multicomponent reaction for the combinatorial synthesis of fused 3-aminoimidazoles. *Angew. Chem., Int. Ed.* **1998**, *37* (16), 2234–2237. (c) Groebke, K.; Weber, L.; Mehlin, F. Synthesis of imidazo[1,2-*a*] annulated pyridines, pyrazines and pyrimidines by a novel three-component condensation. *Synlett* **1998**, *6*, 661–663.

(8) Kercher, T.; Rao, C.; Bencsik, J. R.; Josey, J. A. Diversification of the three-component coupling of 2-aminoheterocycles, aldehydes, and isonitriles: efficient parallel synthesis of a diverse and druglike library of imidazo- and tetrahydroimidazo[1,2-*d*] heterocycles. *J. Comb. Chem.* **2007**, *9* (6), 1177–1187.

(9) Surry, D. S.; Buchwald, S. L. Biaryl phosphane ligands in palladium-catalyzed amination. *Angew. Chem., Int. Ed.* **2008**, *47* (34), 6338–6361.

(10) (a) Fidock, D. A.; Rosenthal, P. J.; Croft, S. L.; Brun, R.; Nwaka, S. Antimalarial drug discovery: efficacy models for compound screening. *Nat. Rev. Drug Discovery* **2004**, *3* (6), 509–520. (b) Vennerstrom, J. L.; Arbe-Barnes, S.; Brun, R.; Charman, S. A.; Chiu, F. C.; Chollet, J.; Dong, Y.; Dorn, A.; Hunziker, D.; Matile, H.; McIntosh, K.; Padmanilayam, M.; Santo Tomas, J.; Scheurer, C.; Scorneaux, B.; Tang, Y.; Urwyler, H.; Wittlin, S.; Charman, W. N. Identification of an antimalarial synthetic trioxolane drug development candidate. *Nature* **2004**, *430* (7002), 900–904.

(11) Trager, W.; Jensen, J. B. Human malaria parasites in continuous culture. *Science* **1976**, *193* (4254), 673–675.

(12) (a) Obach, R. S. Prediction of human clearance of twenty-nine drugs from hepatic microsomal intrinsic clearance data: an examination of in vitro half-life approach and nonspecific binding to microsomes. *Drug Metab. Dispos.* **1999**, *27* (11), 1350–1359. (b) Kalvass, J. C.; Tess, D. A.; Giragossian, C.; Linhares, M. C.; Maurer, T. S. Influence of microsomal concentration on apparent intrinsic clearance: implications for scaling in vitro data. *Drug Metab. Dispos.* **2001**, *29* (10), 1332–1336. (c) Chauret, N.; Gauthier, A.; Nicoll-Griffith, D. A. Effect of common organic solvents on in vitro cytochrome P450-mediated metabolic activities in human liver microsomes. *Drug Metab. Dispos.* **1998**, *26* (1), 1–4. (d) Yan, Z.; Caldwell, G. W. Metabolic assessment in liver microsomes by co-activating cytochrome P450s and UDP-glycosyltransferases. *Eur. J. Drug Metab. Pharmacokinet.* **2003**, *28* (3), 223–232.

(13) (a) Avdeef, A.; Bendels, S.; Di, L.; Faller, B.; Kansy, M.; Sugano, K.; Yamauchi, Y. PAMPA—critical factors for better predictions of absorption. *J. Pharm. Sci.* **2007**, *96* (11), 2893–2909. (b) Avdeef, A. The rise of PAMPA. *Expert Opin. Drug Metab. Toxicol.* **2005**, *1* (2), 325–342.

(14) Balimane, P. V.; Chong, S. Cell culture-based models for intestinal permeability: a critique. *Drug Discovery Today* **2005**, *10* (5), 335–343.

(15) (a) Dubin, A. E.; Nasser, N.; Rohrbacher, J.; Hermans, A. N.; Marrannes, R.; Grantham, C.; Van Rossem, K.; Cik, M.; Chaplan, S. R.; Gallacher, D.; Xu, J.; Guia, A.; Byrne, N. G.; Mathes, C. Identifying modulators of hERG channel activity using the PatchXpress planar patch clamp. *J. Biomol. Screening* **2005**, *10* (2), 168–181. (b) Mathes, C. QPatch: the past, present and future of automated patch clamp. *Expert Opin. Ther. Targets* **2006**, *10* (2), 319–327. (c) Zheng, W.; Spencer, R. H.; Kiss, L. High throughput assay technologies for ion channel drug discovery. *Assay Drug Dev. Technol.* **2004**, *2* (5), 543–552.

(16) Franke-Fayard, B.; Trueman, H.; Ramesar, J.; Mendoza, J.; van der Keur, M.; van der Linden, R.; Sinden, R. E.; Waters, A. P.; Janse, C. J. A *Plasmodium berghei* reference line that constitutively expresses GFP at a high level throughout the complete life cycle. *Mol. Biochem. Parasitol.* **2004**, *137* (1), 23–33.